Stradling, Phys. Letters 6, 143 (1963).

[39] J. M. Chamberlain and R. A. Stradling, Solid State Commun. 7, 1275 (1969).

[40] A. L. Mears and R. A. Stradling, Solid State Commun. 7, 1267 (1969).

[41] J. R. Apel, T. O. Poehler, and C. R. Westgate, Solid State Commun. 8, 1693 (1970).

[42] R. Kubo, S. J. Miyake, and H. Hashitsume, in *Solid State Physics*, Vol. 17, edited by F. Seitz and D. Turnbull (Academic, New York, 1965), p. 269.

[43] H. Kawamura, H. Saji, M. Fukai, K. Sekido, and I. Imai, J. Phys. Soc. Japan 19, 288 (1964).

[44] S. J. Miyake, J. Phys. Soc. Japan 20, 412 (1965).

[45] R. J. Sladek, J. Phys. Chem. Solids 5, 157 (1958); 8, 515 (1959).

[46] Reference 42, p. 255.

[47] R. Kaplan and R. F. Wallis, Phys. Rev. Letters 20, 1499 (1968).

[48] C. J. Summers, R. B. Dennis, B. S. Wherrett, P. G. Harper, and S. D. Smith, Phys. Rev. 170, 755 (1968).

[49] B. D. McCombe and R. Kaplan, Phys. Rev. Letters 21, 756 (1968).

[50] R. C. Enck, A. S. Saleh, and H. Y. Fan, Phys. Rev. 182, 790 (1969).

[51] P. G. Harper, Proc. Phys. Soc. (London) 92, 793 (1967).

PHYSICAL REVIEW B VOLUME 4, NUMBER 2 15 JULY 1971

Electronic Core Levels of the II*B*-VI*A* Compounds

C. J. Vesely* and D. W. Langer

Aerospace Research Laboratories, Wright-Patterson Air Force Base, Ohio 45433

(Received 22 March 1971)

X-ray induced electron-emission measurements were used to determine the energy levels of core electrons in ZnO, ZnS, ZnSe, ZnTe, CdO, CdS, CdSe, CdTe, HgS, HgSe, and HgTe. The investigated energy range extends from the bottom of the valence band to about 1200 eV below the Fermi level. Chemical shifts were determined by comparing our results with experimental values for the pure elements. These shifts are plotted as a function of the fractional ionicity values determined by Phillips and Van Vechten, Pauling, and Coulson. Spin-orbit-splitting values were experimentally determined for the first time for several levels including the Zn3*d*, Cd4*d*, and Hg5*d* levels. Furthermore, our measured energy values for these levels are used to determine the absolute energy values of the initial and final states of transitions normally labeled d_2 in ultraviolet reflectivity and electron-energy-loss measurements. Our results for ZnSe and CdTe are compared with self-consistent relativistic orthogonalized-plane-wave calculations for the excitation energies of these compounds. Agreement with these theoretical calculations is best for the levels closest to the valence band and appears to be angular momentum dependent.

I. INTRODUCTION

The purpose of this paper is to present the results of our x-ray induced electron-emission studies of ZnO, ZnS, ZnSe, ZnTe, CdO, CdS, CdSe, CdTe, HgS, HgSe, and HgTe. The merits of this experimental technique with respect to other procedures such as x-ray absorption and emission, ultraviolet (uv) reflection and absorption, and electron-energy-loss measurements have already been discussed.[1–3]

Section II consists of a description of the experimental procedure. It includes a brief description of the equipment used to make the measurements and a more detailed discussion of the principles of operation as applied to the measurement of semiconductors. This includes a description of the procedures we followed in order to correct for the amount of charge buildup on the samples.

We discuss the results of our measurements in Sec. III which we have divided into four parts. The first part is concerned with the actual location of the energy levels. We list our results and compare them with published experimental data for the pure elements. Our results for ZnSe and CdTe are also compared with theory. In the second part we compare the spin-orbit-splitting values we measured with experimental values for the pure elements and with theoretical values for the elements in the form

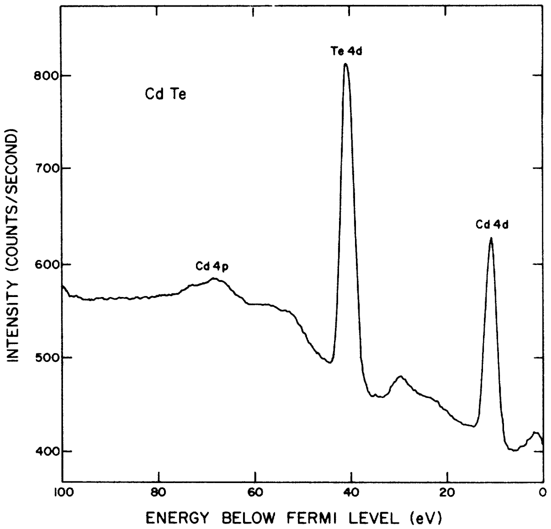

FIG. 1. Electron-emission spectrum of CdTe. The range of binding energies extends from the Fermi level to 100 eV below the Fermi level.

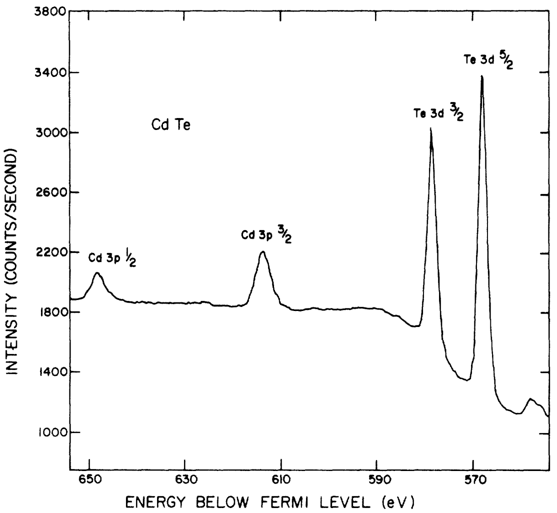

FIG. 2. Electron-emission spectrum of CdTe. The range of binding energies extends from about 560 to 660 eV below the Fermi level.

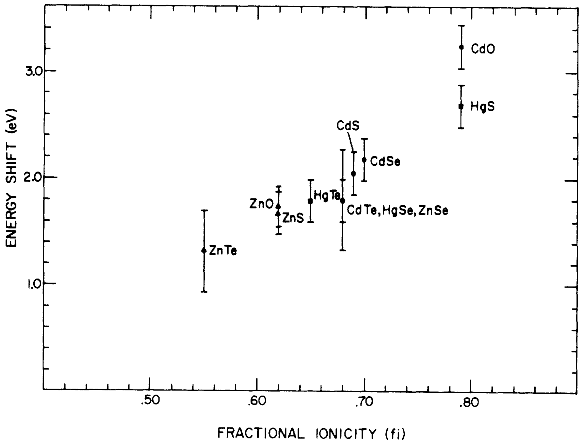

FIG. 4. Energy shifts of the least-bound core levels plotted as a function of the fractional ionicities determined by the theory of Phillips and Van Vechten. The energy shifts for the Zn and Hg compounds are normalized to the value obtained for CdTe.

of free atoms. We also compare our values for ZnSe and CdTe with theoretical calculations for these compounds. The third part concerns the fractional ionicity of the measured crystals. We attempt to correlate the magnitude of the chemical shifts we observed with the fractional ionicity values determined by the three theories of Phillips and Van Vechten, Pauling, and Coulson. The last part of Sec. III concerns the upper *d* bands of the measured compounds. We use the values we obtained for these levels to clarify and extend the interpretation of data obtained by uv reflectivity and electron-energy-loss measurements. The principal results of our measurements are summarized in Sec. IV.

II. EXPERIMENTAL PROCEDURE

A. Apparatus

Our measurements were made with a Varian Associates induced-electron-emission (IEE) spectrometer equipped with a spherical electrostatic electron analyzer[4] and an aluminum x-ray anode. An analyzer potential of 100 V was used yielding an effective resolution of 1.75 eV full width at half-max-

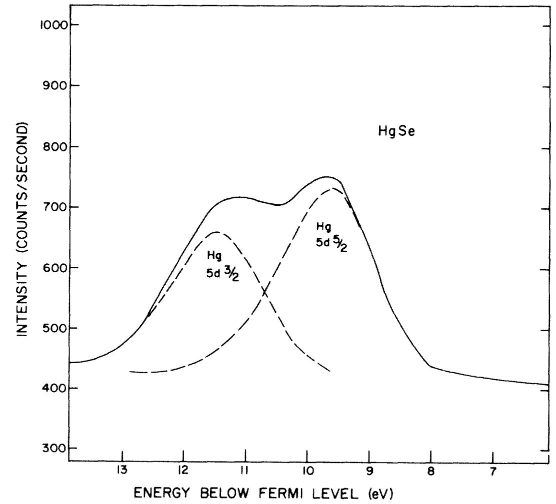

FIG. 3. Electron-emission spectrum of HgSe. The spectrum extends from 6 to 14 eV below the Fermi level. The peaks which were resolved with the Dupont curve resolver are shown in the figure with dashed lines.

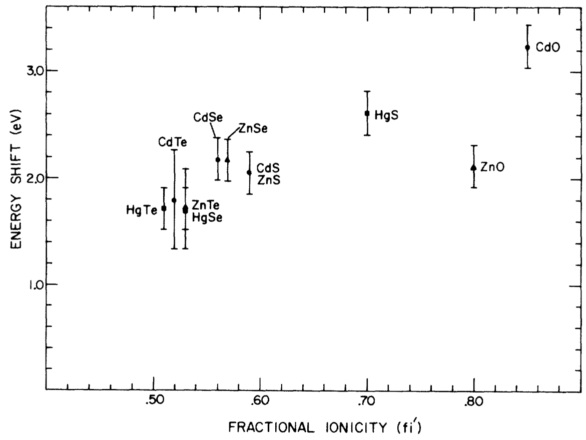

FIG. 5. Energy shifts of the least-bound core levels plotted as a function of the fractional ionicities determined by the theory of Pauling. The Zn and Hg values are normalized to the value obtained for CdS.

TABLE I. Electronic core levels of Zn in metallic Zn and in the measured Zn compounds. Energy values are in eV and are given with respect to the Fermi level of each material. The differences between the measured values for the compounds and the values for the metal are listed in the columns headed by a Δ.

Level	ZnO[a]	Δ[b]	ZnS[a]	Δ[b]	ZnSe[a]	Δ[b]	ZnTe[a]	Δ[b]	Zn metal[c]
$3d_{5/2}$	10.04		10.05		10.09		9.66 ± 0.37		
		(2.24)		(2.17)		(2.29)		(1.83)	8.1 ± 0.6
$3d_{3/2}$	10.79 ± 0.27		10.61		10.85 ± 0.26		10.35 ± 0.40		
$3p_{3/2}$	88.82		89.00		88.99		88.69		
		(3.25)		(3.45)		(3.47)		(3.15)	86.6 ± 0.6
$3p_{1/2}$	91.92 ± 0.23		92.15		92.22		91.86		
$3s$	139.60	3.70	139.96	4.06	139.84	3.94	139.80	3.90	135.9 ± 1.1
$2p_{3/2}$	1021.38 ± 0.21	1.68	1021.65	1.95	1021.54 ± 0.21	1.84	1021.29 ± 0.24	1.59	1019.7 ± 0.6
$2p_{1/2}$	1044.46 ± 0.21	1.66	1044.73	1.93	1044.64	1.84	1044.36 ± 0.27	1.56	1042.8 ± 0.6
$2s$	1195.11	1.51	1195.69	2.09	1195.39	1.79	1195.06	1.46	1193.6 ± 0.9

[a] Present work on Zn compounds.

[b] Those values enclosed by parentheses were calculated by taking the difference between the weighted average of the measured values for a compound and the value for the metal.

[c] From a tabulation of experimental data in Ref. 6.

imum for the carbon 1*s* peak in graphite. A retarding potential was applied between the sample and the entrance slits of the electron analyzer in order to select the electron energy to be analyzed. Most of our measurements were made by sweeping this retarding voltage in 0.1-V increments over a range of 8 to 16 V centered on the region of interest. This procedure would normally be repeated from 40 to 1000 times at a rate of 20 to 80 sec per scan.

The apparatus is equipped with a liquid-nitrogen-trapped mechanical forepump and a titanium sublimation pump. During normal operation the mechanical pump is only used to evacuate the sample entrance chamber. Every effort is taken to prevent hydrocarbon contamination of the main chamber which is maintained at a pressure in the mid 10^{-6}-Torr range during measurements.

B. Principles of Operation

The principles of operation have been previously described.[1] 1486.6-eV x rays from the aluminum x-ray anode interact photoelectrically with electrons in the sample. These electrons are emitted from the sample with a kinetic energy $E_{\text{kin}'}$ which depends on the x-ray energy $E_{\text{x ray}}$, the electron binding energy E_b, and the work function ϕ_s of the sample. If the sample is not a conductor, an additional term ϕ must be included to account for the effect of charge build-up on the sample. The equation that describes the process can then be written as

$$E_b = E_{\text{x ray}} - E_{\text{kin}'} - \phi_s - \phi . \qquad (1)$$

The kinetic energy E_{kin} which is actually measured by the spectrometer is related to $E_{\text{kin}'}$ by

TABLE II. Electronic core levels of Cd in metallic Cd and in the measured Cd compounds. Energy values are in eV and are given with respect to the Fermi level of each material. The differences between the measured values for the compounds and the values for the metal are listed in the columns headed by a Δ.

Level	CdO[a]	Δ[b]	CdS[a]	Δ[b]	CdSe[a]	Δ[b]	CdTe[a]	Δ[b]	Cd metal[c]
$4d_{5/2}$	12.20		11.05		11.13		10.76 ± 0.43		
		(3.24)		(2.05)		(2.18)		(1.79)	9.3 ± 0.3
$4d_{3/2}$	13.06 ± 0.31		11.81		12.00 ± 0.28		11.59 ± 0.57		
$4p$	70.21	3.31	68.76	1.86	68.86	1.96	68.29	1.39	66.9 ± 0.4
$4s$	110.94	3.34	109.65	2.05	109.78	2.18	109.40	1.80	107.6 ± 0.3
$3d_{5/2}$	406.30 ± 0.23	2.60	405.00	1.30	405.13	1.43	404.74	1.04	403.7 ± 0.3
$3d_{3/2}$	413.08	2.50	411.80	1.30	411.93	1.43	411.57	1.07	410.5 ± 0.3
$3p_{3/2}$	619.45	2.95	618.00	1.50	617.96	1.46	617.75 ± 0.25	1.25	616.5 ± 0.3
$3p_{1/2}$	653.81	3.11	652.20	1.50	652.10	1.40	651.90	1.20	650.7 ± 0.3
$3s$	772.91	2.67	771.63	1.43	771.63 ± 0.58	1.43	771.36	1.16	770.2 ± 0.3

[a] Present work on Cd compounds.

[b] Those values enclosed by parentheses were calculated by taking the difference between the weighted average of the measured values for a compound and the value for the metal.

[c] From a tabulation of experimental data in Ref. 6.

TABLE III. Electronic core levels of Hg in metallic Hg and in the measured Hg compounds. The energy values are in eV and are given with respect to the Fermi level of each material. The differences between the measured values for the compounds and the values for the metal are listed in the columns headed by a Δ.

Level	HgS[a]	Δ[b]	HgSe[a]	Δ[b]	HgTe[a]	Δ[b]	Hg metal[c]
$5d_{5/2}$	8.48	(2.80)	7.58	(1.90)	7.53	(1.90)	6.4 ± 1.4
$5d_{3/2}$	10.27		9.39		9.44		
$5p_{3/2}$	65.29	7.69	65.15	7.55	64.33	6.73	57.6 ± 1.3
$5p_{1/2}$	84.50	4.50	83.51	3.01	83.32	2.82	80.5 ± 1.3
$4f_{7/2}$	100.55	2.05	99.50	1.00	99.61	1.11	98.5 ± 0.5
$4f_{5/2}$	104.61	2.41	103.57	1.37	103.68	1.48	102.2 ± 0.5
$4d_{5/2}$	359.48	−0.32	358.62	−1.18	358.75	−1.05	359.8 ± 1.2
$4d_{3/2}$	378.80	0.50	377.98	−0.29	377.98	−0.32	378.3 ± 1.0
$4p_{3/2}$	577.14	6.14	575.89	4.89	577.00	6.00	571.0 ± 1.4
$4p_{1/2}$	680.17	3.27	679.47	2.57	679.93	2.83	676.9 ± 2.4
$4s$	803.16	2.86	802.22	1.92	⋯	⋯	800.3 ± 1.0

[a] Present work on Hg compounds.

[b] Those values enclosed by parentheses were calculated by taking the difference between the weighted average of the measured values for a compound and the value for the metal.

[c] From a tabulation of experimental data in Ref. 6.

$$E_{\text{kin}} = E_{\text{kin}'} + (\phi_s - \phi_{sp}), \tag{2}$$

where ϕ_{sp} is the work function of the electron-analyzer material (oxidized copper). Using this equation, Eq. (1) can be written in terms of E_{kin} as

$$E_b = E_{x\,\text{ray}} - E_{\text{kin}} - \phi_{sp} - \phi . \tag{3}$$

This equation shows that in order to determine the binding energy E_b of the electrons with respect to the Fermi level of the sample, it is necessary, in addition to measuring E_{kin}, to determine the values of ϕ_{sp} and ϕ. While ϕ_{sp} is a constant for the system and therefore need only be determined once, the quantity ϕ must be determined for each sample since it depends on the conductivity of the material

TABLE IV. Electronic core levels of O, S, Se, and Te in the measured compounds and in the pure materials. The energy values are in eV and are given with respect to the Fermi level of each material. The differences between the measured values for the compounds and the values for the pure materials are listed in the columns headed by a Δ.

Level	Zn(x)[a]	Δ[b]	Cd(x)[a]	Δ[b]	Hg(x)[a]	Δ[b]	(x)[c]
O 1s	530.60	−1.40	531.28 ± 0.27	−0.72	⋯	⋯	532.0 ± 0.4
S $2p_{3/2}$	161.71	(−2.74)	161.60	(−2.82)	161.44	(−2.96)	164.8 ± 0.7
S $2p_{1/2}$	162.75		162.74		162.63		
S 2s	225.97	−3.23	225.84	−3.36	225.76	−3.44	229.2 ± 0.4
Se $3d_{5/2}$	54.02	(−2.30)	54.18	(−2.15)	53.26	(−3.14)	56.7 ± 0.8
Se $3d_{3/2}$	54.97		55.07		54.00		
Se $3p_{3/2}$	160.23	−1.67	160.32	−1.58	159.59	−2.31	161.9 ± 1.0
Se $3p_{1/2}$	166.07	−2.13	166.04	−2.16	165.40	−2.80	168.2 ± 1.3
Se 3s	229.09	−2.41	228.96	−2.54	228.46	−3.04	231.5 ± 0.7
Te $4d_{5/2}$	39.97 ± 0.29	(0.77)	39.92 ± 0.31	(0.72)	39.61	(0.37)	39.8 ± 0.3
Te $4d_{3/2}$	41.47 ± 0.24		41.42 ± 0.25		41.12		
Te 4s	168.80	0.50	168.77	0.47	168.11	−0.19	168.3 ± 0.3
Te $3d_{5/2}$	572.16	0.06	572.11 ± 0.23	0.01	571.88	−0.22	572.1 ± 0.3
Te $3d_{3/2}$	582.56	0.06	582.54	0.04	582.39	−0.11	582.5 ± 0.3
Te $3p_{3/2}$	818.75	0.05	818.74	0.06	818.58	−0.12	818.7 ± 0.3
Te $3p_{1/2}$	869.63	−0.07	869.52	−0.18	869.47	−0.23	869.7 ± 0.3
Te 3s	1005.48	−0.52	1005.39	−0.61	1004.60	−1.40	1006.0 ± 0.3

[a] Present work on the II-VI compounds. The (x) represents O, S, Se, or Te.

[b] Same as footnote b for Table I.

[c] Same as footnote c for Table I.

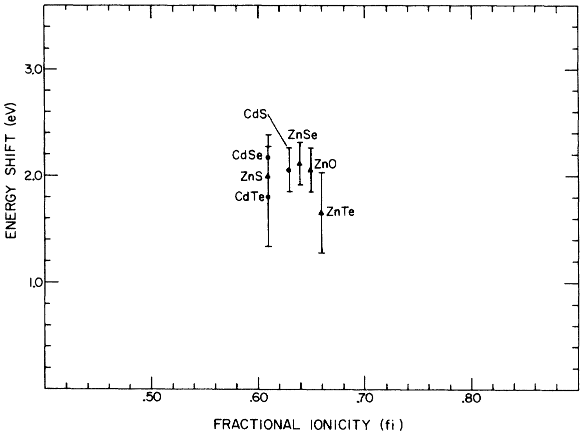

FIG. 6. Energy shifts of the least-bound core levels plotted as a function of the fractional ionicities determined by the theory of Coulson. The Zn values are normalized to the values obtained for CdSe and CdTe.

being measured.

We have chosen to combine ϕ_{sp} and ϕ and remeasure this total quantity for each new material measured. We do this by depositing from a candle flame a thin coating of carbon on at least one sample of each material measured. Our samples are prepared by crushing the material to be measured and attaching it to an aluminum sample holder with scotch tape. For the carbon-coated sample we measure the C 1*s* line and one or more of the strongest lines in the sample material. We then compare the observed value for the C 1*s* line to the reported value of 283.8 eV[5] for carbon prepared in a similar manner. The difference between these two values is equal to $\phi_{sp}+\phi$, and we apply this quantity to the measured sample lines in order to obtain their absolute values. We then use these lines as our reference lines for this material in order to correct the remaining energy-level values which are measured in samples prepared without the carbon layer. The assumption here is that ϕ is the same for both the thin layer of carbon and the surface layer of the sample which is being penetrated by the x rays. From the scatter in our measurements we estimate that this technique allows us to determine the peak locations to within ± 0.2 eV (not including systematic errors). Most lines were measured at least twice apiece for three or more samples. The calculated standard deviation (σ) is shown in the tables for those levels where the scatter in measurements yielded a value greater than ± 0.2 eV. Otherwise, the value is omitted and σ is assumed to be ± 0.2 eV. The measured differences between energy levels of the same compound, however, are not affected by charge buildup on the samples so they should be accurate to within ± 0.1 eV.

III. DISCUSSION OF RESULTS

A. Electron Core Levels

Figures 1 and 2 are typical examples of x-ray-induced photoemission spectra. Figure 1 shows the photoelectron distribution for a range of binding energies extending from the Fermi level to 100 eV below the Fermi level for CdTe. The dominant peaks are easily identified with the corresponding atomic

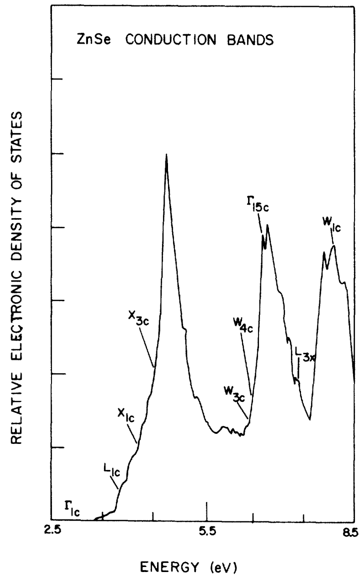

FIG. 7. Calculated density-of-states distribution for the conduction band of ZnSe. The drawing is taken from a paper by Stukel, Collins, and Euwema (Ref. 19) and is based on the results of their self-consistent orthogonalized-plane-wave calculations.

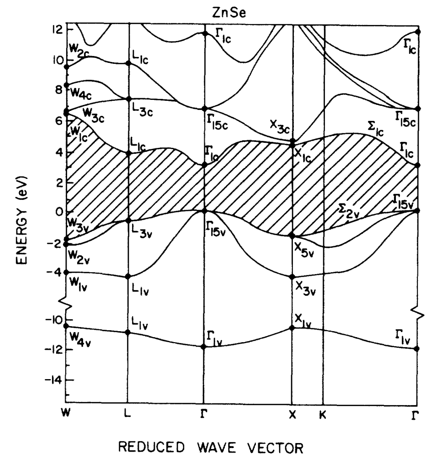

FIG. 8. Calculated band structure of ZnSe. The drawing is taken from a paper by Stukel, Collins, and Euwema (Ref. 19) and is based on the results of their self-consistent orthogonalized-plane-wave calculations.

TABLE V. Electronic core levels of Zn and Se in ZnSe. The table lists our experimental values and the values obtained by SCROPW calculations of Collins, Wepfer, and Euwema (Ref. 7). The experimental values are given with respect to the Fermi level and the theoretical values are given with respect to the center of the band gap.

	Zinc				Selenium	
Expt	Theor	Δ	Level	Expt	Theor	Δ
10.09	9.88	−0.21	$3d_{5/2}$	54.02	55.02	1.00
10.85	10.28	−0.57	$3d_{3/2}$	54.97	55.99	1.02
88.99	83.98	−5.01	$3p_{3/2}$	160.23	154.77	−5.46
92.22	87.17	−5.05	$3p_{1/2}$	166.07	160.90	−5.17
139.84	130.87	−8.97	$3s$	229.09	217.24	−11.85
1021.54	1019.25	−2.29	$2p_{3/2}$	···	···	
1044.64	1043.86	−0.78	$2p_{1/2}$	···	···	
1195.39	1177.78	−17.61	$2s$	···	···	

core levels as indicated in the figure. The Cd $4d$ and $4p$ levels are shown along with the Te $4d$ level. The valence band structure between the Cd $4d$ level and the Fermi level is poorly resolved and much less intense than the core-level peaks. This is due to the 1.75-eV resolution of the system and the relatively low density of states in the valence band region when compared to the core levels. Also, the probability of interaction between the 1486-eV x ray and the electrons in a material decreases with decreasing electron binding energy.

Figure 2 shows another photoemission spectrum for CdTe. This one extends from about 560 to 660 eV below the Fermi level and shows both the Cd $3p$ doublet and Te $3d$ doublet. The spin-orbit splitting for both these doublets is quite large compared to the resolution of the system so there is no problem in accurately determining its magnitude. For levels that were split by less than 2 eV, however, it was necessary to use a Dupont curve resolver in order to determine the binding energy of each peak in the doublet. Two single peaks due to the C 1s line in amorphous carbon and obtained at the same spectrometer resolution were used as the starting point in these analyses. Height, width, skew, and position were independently adjusted for each of the two reference peaks in order to obtain the best fit. Figure 3 illustrates the results of this procedure by showing a spectrum we obtained for HgSe. The spectrum extends from 6 to 14 eV below the Fermi level and includes the Hg $5d$ doublet. The peaks that we were able to resolve with the curve resolver are also shown in the figure.

The results of our measurements are shown in Tables I–IV. These tables list the values that we were able to obtain for zinc (these values differ from those presented in Ref. 1 because of the following two reasons: The previous values included a systematic error of about 1 eV due to the use of a C 1s reference value which did not correspond to the C 1s line which was being measured; in addition, small changes in either direction resulted from using the improved method of correcting for charge buildup on the samples), cadmium, mercury, oxygen, sulfur, selenium, and tellurium electron-core levels in the compounds along with experimental values for the pure elements as reported in the table of electron energy levels compiled by Bearden and Burr.[6] All values are given with respect to the Fermi level of the material measured. All the zinc, cadmium, and mercury levels in the compounds with the exception of the Hg $4d$ levels have shifted toward higher binding energies compared to the pure elements. This was expected and can be explained by considering the partial ionic character of the bonding in these crystals. The metal atoms lose some electronic charge in the bonding and consequently become positively charged. The result is a slight contraction of the electron distribution about the nucleus or an increase in binding energy. The reverse is true for the oxygen, sulfur, selenium, and tellurium atoms. Here, the atoms gain electronic charge because of the ionic bonding in the crystals, and the result is an expansion in the electron distribution or a decrease in binding energy. This is the result we observed for the oxygen, sulfur, and selenium levels. However, our results for tellurium (small positive and negative shifts) lead us to believe that the reported values for tellurium metal may be 1–3 eV too small. Also, by looking at the magnitude of the shift between the values we measured for Hg in the compounds and the reported values for Hg, it appears that reported values for the $4d$ doublet and both the

TABLE VI. Electronic core levels of Cd and Te in CdTe. The table lists our experimental values and the values obtained by the SCROPW calculations of Collins, Wepfer, and Euwema (Ref. 8). The experimental values are given with respect to the Fermi level and the theoretical values are given with respect to the center of the band gap. All values are in eV.

	Cadmium				Tellurium	
Expt	Theor	Δ[a]	Level	Expt	Theor	Δ
10.76	10.52	−0.24	$4d_{5/2}$	39.92	40.13	0.21
11.59	11.29	−0.30	$4d_{3/2}$	41.42	41.71	0.29
	65.71		$4p_{3/2}$	···	111.89	···
68.29		(−0.99)				
	71.81		$4p_{1/2}$	···	122.03	···
109.40	106.15	−3.25	$4s$	168.77	165.41	−3.36
404.74	406.14	1.40	$3d_{5/2}$	572.11	573.57	1.46
411.57	413.44	1.87	$3d_{3/2}$	582.54	584.70	2.16
617.75	606.00	−11.75	$3p_{3/2}$	818.74	805.78	−12.96
651.90	641.38	−10.52	$3p_{1/2}$	869.52	858.30	−11.22
771.36	748.20	−23.66	$3s$	1005.39	982.35	−23.04

[a] The value enclosed by parentheses was calculated by taking the difference between the weighted average of the calculated values and the measured value.

TABLE VII. Measured spin-orbit-splitting values for Zn, Cd, and Hg. The table also includes experimental values for the pure elements from the table of electron binding energies compiled by Bearden and Burr and theoretical values obtained by Herman and Skillman. All values are in eV.

Level	O[a]	S[a]	Se[a]	Te[a]	Metal[b]	Free atom[c]
Zn3*d*	0.75 ± 0.20	0.56 ± 0.10	0.76 ± 0.23	0.69 ± 0.10	...	0.40
Zn3*p*	3.10 ± 0.14	3.15 ± 0.10	3.23 ± 0.10	3.17 ± 0.11	...	3.09
Zn2*p*	23.08 ± 0.10	23.05 ± 0.10	23.10 ± 0.10	23.07 ± 0.10	23.1 ± 0.9	23.92
Cd4*d*	0.86 ± 0.22	0.76 ± 0.12	0.87 ± 0.16	0.83 ± 0.20	...	0.79
Cd3*d*	6.78 ± 0.10	6.80 ± 0.10	6.80 ± 0.10	6.83 ± 0.10	6.8 ± 0.4	7.32
Cd3*p*	34.36 ± 0.10	34.20 ± 0.10	34.17 ± 0.10	34.15 ± 0.10	34.2 ± 0.4	32.55
Hg5*d*	...	1.79 ± 0.10	1.81 ± 0.10	1.91 ± 0.10	...	2.11
Hg5*p*	...	19.21 ± 0.10	18.36 ± 0.10	18.99 ± 0.10	22.9 ± 1.8	14.41
Hg4*f*	...	4.06 ± 0.10	4.07 ± 0.10	4.07 ± 0.10	3.7 ± 0.7	4.74
Hg4*d*	...	19.32 ± 0.10	19.36 ± 0.10	19.23 ± 0.12	18.5 ± 1.6	19.47
Hg4*p*	...	103.03 ± 0.20	103.58 ± 0.20	102.55 ± 0.20	105.9 ± 2.8	81.29

[a] Present work on II-VI compounds. [b] Reference 6. [c] Reference 10.

$5p3/2$ and $4p3/2$ levels may be in error. The values for the doublet should be decreased by 1.5 to 3 eV and the values for the $p3/2$ levels should be increased by about 3 eV.

Excitation energies for ZnSe[7] and CdTe[8] have been calculated by Collins, Wepfer, and Euwema with a self-consistent relativistic orthogonalized-plane-wave method (SCROPW). These are the energies which are required to excite electrons within these materials to some arbitrary reference level. After shifting this reference level to the Fermi level, the results of their calculations should be directly comparable with our data. In their model, the exchange-correlation-relaxation operator is approximated by a constant (α) times Slater's free-electron exchange operator. This is a simplification of the model in which the excitation Hamiltonian is an energy-dependent functional of the electron density.[7] Nevertheless, the results they obtained for ZnSe indicate that good approximate excitation energies may be obtained with the proper choice of α. The approximation, however, is best for energies at or near the Fermi surface.[9]

Tables V and VI list our experimental values for the Zn and Se levels in ZnSe and the Cd and Te levels in CdTe along with the excitation energies calculated by the SCROPW method of Collins, Wepfer, and Euwema. As expected, the differences between the measured and calculated values are in general smallest for the levels closest to the Fermi level. In addition, however, agreement appears to be best for the *d* states, not as good for the *p* states and worst for the *s* states.

B. Spin-Orbit Splitting

We were able to determine the spin-orbit splitting for many of the levels that we measured. The values we obtained are listed in Tables VII and VIII along with experimental values from the table of electron binding energies compiled by Bearden and Burr. Tables VII and VIII also include theoretical values for the free atoms obtained by Herman and Skillman[10] using a first-order perturbation treatment. Strict agreement with these theoretical values was not expected because Herman *et al.*[11] stated that their perturbation treatment was not entirely adequate and that a change in the splitting would be caused by wave-function renormalization effects when going from the free atom to a crystalline configuration. In comparing our values with these theoretical calculations we find relatively good agreement, however, for all the levels except for the Cd 3*p*, Hg 5*p*, Hg 4*p*, and Te 3*p* levels. Tables IX and X show our data for ZnSe and CdTe along with the values predicted by the SCROPW calculations of Collins, Wepfer, and Euwema. Their values are almost the same as the Herman and Skillman values except for the 3*p* levels where they predict splittings which are larger than the Herman and

TABLE VIII. Measured spin-orbit-splitting values for S, Se, and Te. The table also includes experimental values for the pure elements from the table of electron binding energies compiled by Bearden and Burr and theoretical values obtained by Herman and Skillman. All values are in eV.

Level	Zn[a]	Cd[a]	Hg[a]	Pure[b] element	Free[c] atom
S2*p*	1.04 ± 0.10	1.14 ± 0.10	1.19 ± 0.10	...	1.35
Se3*d*	0.95 ± 0.19	0.89 ± 0.10	0.74 ± 0.10	...	0.99
Se3*p*	5.84 ± 0.15	5.72 ± 0.10	5.81 ± 0.10	6.3 ± 1.6	5.88
Te4*d*	1.50 ± 0.10	1.50 ± 0.10	1.51 ± 0.10	...	1.61
Te3*d*	10.40 ± 0.10	10.43 ± 0.10	10.51 ± 0.10	10.4 ± 0.4	11.12
Te3*p*	50.88 ± 0.10	50.78 ± 0.10	50.89 ± 0.13	51.0 ± 0.4	47.61

[a] Present work on the II-VI compounds.
[b] Reference 6.
[c] Reference 10.

TABLE IX. Spin-orbit-splitting values for Zn and Se in ZnSe. The table lists our experimental values and the values obtained by the SCROPW calculations of Collins, Wepfer, and Euwema (Ref. 7). All values are in eV.

Zinc				Selenium		
Expt	Theor	Δ	Level	Expt	Theor	Δ
0.76 ± 0.23	0.40	−0.36	$3d$	0.95 ± 0.19	0.97	0.02
3.23 ± 0.10	3.19	−0.04	$3p$	5.84 ± 0.15	6.13	0.29
23.10 ± 0.10	24.61	1.51	$2p$	...	...	...

Skillman values. Where the Herman and Skillman values were 1–3 eV smaller than our observed values for Cd and Te, the SCROPW values are 1–2 eV larger.

For those levels which had previously been measured and which were listed in Bearden and Burr's table of electron binding energies we see from Tables VII and VIII that agreement with our data is extremely good except for the Hg $4p$ and $5p$ levels. This agrees with our previous conclusion that the reported values for the Hg $4p$ 3/2 and $5p$ 3/2 levels may be in error. Our values for the S $2p$ level agree very well with the value of 1.2 eV reported by Lindberg *et al.*[12]

We were unable to detect any significant variation among the compounds in the magnitude of the splittings. This was even true for the upper *d* bands where some contribution due to crystal-field splitting could be expected.

C. Ionicity

Although the shifts we observed in energy levels between the various related compounds are small, we have made an attempt to correlate them with the reported fractional ionicity values for these materials. In Figs. 4–6 we have plotted the shifts in the least bound core levels as a function of the fractional ionicities determined by the theories of Phillips and Van Vechten,[13,14] Pauling,[15,16] and Coulson.[17] In each figure, we have normalized the Zn and Hg energy-shift values to the values obtained for Cd. For example, Phillips and Van Vechten calculate a fractional ionicity of 0.68 for CdTe, ZnSe, and HgSe for which we obtained energy-shift values of 1.79, 2.29, and 1.90 eV, respectively. We feel that the differences in these energy shifts could easily be accounted for by the experimental uncertainties of 0.3 to 2.0 eV in the values compiled by Bearden and Burr for the outer levels of Zn, Cd, and Hg. We have therefore subtracted 0.5 eV from the energy shifts we obtained for the four Zn compounds and 0.11 eV from the values we obtained for the three Hg compounds in order to make the values for CdTe, ZnSe, and HgSe agree. The results are plotted in Fig. 4 and demonstrate a strong correlation between the normalized energy shifts and the calculated ionicity values. We followed the same procedure for Pauling's theory which predicts the same ionicity value for both ZnS and CdS. The results are shown in Fig. 5. According to Coulson's theory, CdSe, CdTe, and ZnS should all have a value of 0.61. We shifted the Zn values so that ZnS would have the same energy-shift value as the average of the CdSe and CdTe values. These results are shown in Fig. 6.

From Tables I–IV it is apparent that the magnitude of the shift between the values we observed and the pure materials is, in general, a function of the principal quantum number. For Zn, Cd, and Hg the larger shifts occurred for the outer levels while for Te the reverse appears to be true. This is contrary to the experimental results obtained by Fadley and Shirley[18] who observed the same amount of shift for all levels in a series of iodine compounds. In addition, Hartree-Fock-type calculations that were performed by these authors to determine the binding energy shifts due to removing a $5p$ electron from various free-ion configurations also predicted that all core levels would shift by about the same amount. We feel that the difference we see in the magnitude of the shifts as a function of the principal quantum number may be the result of an energy-dependent relaxation effect. This agrees with the previously mentioned model that employs an exchange-correlation–relaxation operator which is an energy-dependent functional of the charge density.

D. Zn 3*d*, Cd 4*d*, and Hg 5*d* Levels

The Zn $3d$, Cd $4d$, and Hg $5d$ levels lie so close in energy to the valence bands of their respective compounds that they exert a much stronger influence on the structure of the valence band then the deeper-lying core levels. Consequently, their exact positions with respect to the structure in the valence and conduction bands are probably of more interest than the lower levels to band-structure theoreticians. We therefore look at these upper *d* bands in more detail.

Several different experimental techniques which are normally used to study the structure of the valence and conduction bands have been used to determine or estimate the location of the upper *d* bands.

TABLE X. Spin-orbit-splitting values for Cd and Te in CdTe. The table lists our experimental values and the values obtained by the SCROPW calculations of Collins, Wepfer, and Euwema (Ref. 8). All values are in eV.

Cadmium				Tellurium		
Expt	Theor	Δ	Level	Expt	Theor	Δ
0.83 ± 0.20	0.77	−0.06	$4d$	1.50 ± 0.10	1.58	0.08
6.83 ± 0.10	7.30	0.47	$3d$	10.43 ± 0.10	11.13	0.70
34.15 ± 0.10	35.38	1.23	$3p$	50.78 ± 0.10	52.52	1.74

TABLE XI. Comparison of experimental results for the Zn3*d*, Cd4*d*, and Hg5*d* levels. All values are given with respect to the center of the energy gap (or Fermi level for our data) and are in eV. The values in parentheses include a correction for the energy difference between the L_{1c} point and the bottom of the conduction band. The band-gap energies used for adjustment are ZnO, 3.4 eV; ZnS, 3.8 eV; ZnSe, 2.8 eV; ZnTe, 2.4 eV; CdS, 2.5 eV; CdSe, 1.8 eV; CdTe, 1.6 eV; HgSe, 0 eV; and HgTe, 0 eV.

Compound	x-ray[a] electron emission	uv electron emission	uv reflectivity	Electron energy loss
ZnO	10.34 ± 0.20	...	16.3[b] (9.8)[c] 16.3[d] (9.8)[c]	17.1[b] (11.4)[c]
ZnS	10.27 ± 0.20	...	12.1[e] (10.3)[f] 11.9[h] (10.1)[f]	13.2[g] (11.4)[f]
ZnSe	10.39 ± 0.20	...	12.4[e] (10.6)[f]	13.5[g] (11.7)[f]
ZnTe	9.93 ± 0.38	...	13.4[i] (12.3)[f] 13.4[j] (12.3)[f]	12.6[i] (11.5)[f] 12.7[g] (11.6)[f]
CdS	11.35 ± 0.20	10.7 ± 0.5[m]	13.1[k] (10.9)[l] 13.2[e] (11.0)[l] 12.7[h] (10.5)[l]	13.2[g] (11.0)[l]
CdSe	11.48 ± 0.20	...	13.5[e] (11.6)[l] 13.1[h] (11.2)[l]	13.3[g] (11.4)[l]
CdTe	11.09 ± 0.48	11.1[n]	13.0[j] (11.4)[f]	...
HgSe	7.58 9.39	... ...	9.7[o] (7.6)[p] 11.1[o] (9.0)[p]	...
HgTe	7.53	...	9.55[o] (7.85)[p] 9.7[j] (8.0)[p]	...
	9.44	...	11.1[o] (9.4)[p] 11.3[j] (9.6)[p]	...

[a] Present work on II-VI compounds. Values listed for the Zn and Cd compounds are weighted averages of the doublets.

[b] Reference 24. This value is the high-energy portion of the observed structure.

[c] The *L*-Γ energy difference was taken from Ref. 20.

[d] Y. Park, T. Wagner, H. Nalkowski, M. Skibowski, and R. Klucker, DESY Report No. 70/9, 1970 (unpublished). This value is the high-energy portion of the observed structure.

[e] M. Balkanski and Y. Petroff, in *Proceedings of the Seventh International Conference on Semiconductors, Paris*, 1964, edited by M. Hulin (Dunod Cie., Paris, 1964), p. 245

[f] The *L*-Γ energy difference is the average of the values obtained from Refs. 21 and 22.

[g] T. Tomoda and M. Mannami, J. Phys. Soc. Japan 27, 1204 (1969).

[h] M. Cardona and G. Harbeke, Phys. Rev. 137, A1467 (1965).

[i] J. Gilbert, R. Hengehold, and F. Pedrotti, Bull. Am. Phys. Soc. 15, 349 (1970).

[j] M. Cardona and D. Greenaway, Phys. Rev. 131, 98 (1963).

[k] W. Walker and J. Osantowski, J. Phys. Chem. Solids 25, 778 (1964).

[l] The *L* - Γ energy difference is the average of the values obtained from Refs. 19 and 22.

[m] N. Kindig and W. Spicer, Phys. Rev. 138, A561 (1965).

[n] J. Shay and W. Spicer, Phys. Rev. 161, 799 (1967).

[o] W. Scouler and G. Wright, Phys. Rev. 133, A736 (1964).

[p] The *L*-Γ energy difference was taken from Ref. 23.

The results of these measurements are listed in Table XI along with weighted averages of the doublets we measured. We were unable to find any experimental values other than our own for CdO and HgS so we have omitted these two compounds from the table. All the values listed in the table have been corrected so that they are given with respect to the center of the band gap and we assume that the Fermi level does not deviate appreciably from the center of the gap. (A discussion of this point is included in our paper on the zinc compounds.[1]) Thus, for uv reflectivity and electron-energy-loss mea-

TABLE XII. Comparison of our results with theoretical calculations for the Zn3*d*, Cd4*d*, and Hg5*d* levels. All values are given with respect to the center of the energy gap (or Fermi level for our data) and are in eV.

Compound	x-ray[a] electron emission	SCROPW	KKR	APW[b], SCOPW[c] EROPW[d]
ZnO	10.04 10.79	...	6.3[e]	...
ZnS	10.05 10.61	...	9.0[e], 8.6[f]	16.1[†g], 6.9[‡g]
ZnSe	10.09 10.85	9.88[h] 10.28[h]	8.9[f]	14.1[†g], 7.7[‡g]
ZnTe	9.66 10.35	...	10.7[f]	12.8[†g]
CdO	12.41 13.28	...	...	7.1[*i]
CdS	11.05 11.81	...	...	17.9[†g], 7.0[‡g]
CdSe	11.13 12.00	...	...	15.6[†g], 7.8[‡g]
CdTe	10.76 11.59	10.52[j] 11.29[j]	12.0[f]	...
HgSe	7.58 9.39	...	9.8[k] 11.7[k]	...
HgTe	7.53 9.44	...	10.4[k] 12.3[k]	...

[a] Present work on II-VI compounds.

[b] Values obtained by augmented-plane-wave calculations are marked with an asterisk.

[c] Values obtained by self-consistent orthogonalized-plane-wave calculations are marked with a dagger.

[d] Values obtained by empirically refined orthogonalized-plane-wave calculations are marked with a double dagger.

[e] Reference 20.

[f] J. Treusch, P. Eckelt, and O. Madelung, in Ref. 22, p. 588.

[g] Reference 19; value for ZnTe (private communication).

[h] Reference 7.

[i] K. Maschke and U. Rössler, Phys. Status Solidi 28, 577 (1968).

[j] Reference 8.

[k] Reference 23.

surements we have subtracted one-half of the band gap from the reported values and for uv-photoemission measurements, which are given with respect to the top of the valence band, we have added one-half the energy gap.

Of the three other techniques, uv photoemission (like x-ray photoemission) is the only method capable of determining the location of the *d* bands unambiguously. The table shows that our values agree very well with the uv-photoemission data, especially for CdTe. The data from uv reflectivity and electron-energy-loss measurements represent transitions of electrons from the *d* band into the conduction band so it is necessary to know the energy of the final states of these transitions in order to pin down the energy of the *d* band. The final states of such transitions would not necessarily be at the bottom of the conduction band but some point above the bottom where a high density of vacant states occurs. This explains why the values obtained by these two techniques are all larger by a few eV than the x-ray and uv-photoemission values.

Figure 7 shows a plot of the calculated density of states for the conduction band of ZnSe. The drawing is taken from a paper by Stukel, Collins, and Euwema[19] and is based on the results of their self-consistent orthogonalized-plane-wave (SCOPW) calculations. The figure shows that the lowest high density-of-states region lies about 0.8 eV above the L_{1c} point. Figure 8 shows a plot of the ZnSe band structure obtained by their calculations. It appears that the above-mentioned peak in the density of states results from the broad nearly flat regions near the L_{1c}, X_{1c}, and X_{3c} points. Some point in this area would then be a good candidate for being the final state of the transitions between the *d* band and conduction band measured by uv reflectivity and electron-energy-loss measurements. In order to test this hypothesis, we obtained from theoretical band-structure calculations[19-23] the energy differences between the L_1 point and the bottom of the conduction band for each of the compounds and subtracted these differences from the uv reflectivity and electron-energy-loss values. The results are the values enclosed by parentheses in Table XI and agree very well with our values. In those cases where the reflectivity and energy-loss values are still larger than ours, the difference can be attributed to the difference between the location of the L_{1c} point and the true location of the lowest maximum in the conduction-band density-of-states distribution.

It has been pointed out by other investigators[24] that the reflectivity of ZnO is different from that of the other II-VI compounds in that the major structure begins beyond 10 eV, whereas in the other II-VI compounds the valence-band transitions are practically exhausted at this energy, and the reflectivity is on a sharp decrease. They conclude from this that the valence bands lie deeper in ZnO than in the other II-VI compounds. However, Rossler's[20] Korringa-Kohn-Rostoker (KKR) calculations for ZnO yield a value of 9.1 eV for the distance between the L_{1c} point and the top of the valence band, compared to typical values of 3 to 5 eV for the other II-VI compounds. On the basis of his calculations, and on the assumption that the uv reflectivity peaks and the electron-energy-loss measurements do indeed represent transitions to the lowest maximum of the conduction-band density-of-states distribution, we would expect a larger difference between the results of those measurements and our own for ZnO than for the other II-VI compounds. From Table XI it can be seen that this was indeed the observed result. Furthermore, this would explain the unique characteristics of the observed ZnO reflectivity and energy-loss spectra when compared with the other II-VI compounds.

Table XII compares our results with values obtained by several different types of theoretical band-structure calculations. We were unable to find any values for HgS. The table shows that the SCROPW values agree best with the experimental values.

IV. CONCLUSION

The results of our x-ray-induced electron-emission studies of the II-VI compounds are summarized.

(i) The deposition of a thin film of carbon on a sample of each material being studied appears to allow the determination of electron binding energies to within ± 0.2 eV for nonconducting materials.

(ii) All the zinc, cadmium, and mercury levels in the compounds with the exception of the Hg 4*d* levels have shifted toward higher binding energies compared to the pure elements. The oxygen, sulfur, and selenium levels shifted toward lower binding energies. Small shifts in both directions were observed for the tellurium levels. All of these shifts with the exception of the Hg 4*d* levels and the tellurium levels can be understood by considering the partial ionic character of the bonding in these crystals.

(iii) Comparison between our measured values and SCROPW excitation energies for ZnSe and CdTe indicates that agreement is in general best for the levels closest to the Fermi level. In addition, agreement appears to be best for the *d* states, not as good for the *p* states, and worst for the *s* states.

(iv) Several spin-orbit splitting values were measured for the first time. Comparison with theoretical calculations for both free atoms and the measured compounds revealed the largest discrepancies for *p* states.

(v) Comparison of energy shifts with fractional ionicity values indicated best agreement with the values predicted by the theory of Phillips and Van Vechten. Contrary to previously reported results which indicated the same amount of shift for all energy levels, we observed different shifts for levels with different principal quantum numbers.

(vi) Comparison of our results for the upper *d* bands with uv reflectivity and electron-energy-loss-measurements indicates that there are peaks in the spectra obtained by these techniques which could represent transitions between the *d* level and the lowest-lying maximum in the conduction-band density-of-states distribution. Theoretical calculations indicate that this point is slightly above the L_{1c} point. This interpretation may explain the difference between the uv-reflectivity spectra obtained for ZnO and the other II-VI compounds.

ACKNOWLEDGMENTS

We wish to thank T. C. Collins and R. L. Hengehold for many helpful discussions and also L. Croft for his technical assistance during the course of this investigation. We also wish to thank T. C. Collins, G. G. Wepfer, R. N. Euwema, and H. Overhof for the communication of their results before publication.

---

*Part of this work has been submitted by C. J. Vesely to the Air Force Institute of Technology, Air University, in partial fulfillment of the requirements for the degree of Doctor of Philosophy.

[1] D. Langer and C. Vesely, Phys. Rev. B 2, 4885 (1970).

[2] K. Siegbahn, C. Nordling, A. Fahlman, R. Nordberg, K. Hamrin, J. Hedman, G. Johansson, T. Bergmark, S.-E. Karlsson, I. Lindgren, and B. Lindberg, Nova Acta Reg. Soc. Sci. Ups. 20, 1 (1967).

[3] D. Hercules, Ann. Chem. 42, 20A (1970).

[4] J. Helmer and N. Weichert, Appl. Phys. Letters 13, 266 (1968).

[5] S. Hagström and S.-E. Karlsson, Arkiv Fysik 26, 451 (1964).

[6] J. Bearden and A. Burr, Rev. Mod. Phys. 39, 125 (1967).

[7] T. Collins, G. Wepfer, and R. Euwema, Intern. J. Quantum Chem. Symposium (to be published).

[8] T. Collins, G. Wepfer, and R. Euwema, Bull. Am. Phys. Soc. 16, 372 (1971).

[9] T. Collins, in Ref. 7; also (private communication).

[10] F. Herman and S. Skillman, *Atomic Structure Calculations* (Prentice-Hall, Englewood Cliffs, N. J., 1963).

[11] F. Herman, C. Kuglin, K. Cuff, and R. Kortum, Phys. Rev. Letters 11, 541 (1963).

[12] B. Lindberg, K. Hamrin, G. Johansson, U. Gelius, A. Fahlman, C. Nordling, and K. Siegbahn, Uppsala University Report No. UUIP-638, 1970 (unpublished).

[13] J. Phillips, Rev. Mod. Phys. 42, 317 (1970).

[14] J. Phillips and J. A. Van Vechten, Phys. Rev. B 2, 2147 (1970).

[15] L. Pauling, *The Nature of the Chemical Bond* (Cornell U. P., Ithaca, N. Y., 1939).

[16] L. Pauling, Phys. Today 24, No. 2, 9 (1971).

[17] C. Coulson, L. Redei, and D. Stocker, Proc. Roy. Soc. (London) 270, 352 (1962).

[18] C. Fadley, S. Hagstrom, M. Klein, and D. Shirley,

J. Chem. Phys. 48, 3779 (1968).

[19] D. Stukel, R. Euwema, T. Collins, F. Herman, and R. Kortum, Phys. Rev. 179, 740 (1969).

[20] U. Rössler, Phys. Rev. 184, 733 (1969).

[21] M. Cohen and T. Bergstresser, Phys. Rev. 141, 789 (1966).

[22] F. Herman, R. Kortum, C. Kuglin, and J. Shay, in *Proceedings of the International Conference of II-VI Semiconducting Compounds*, *Providence*, 1967, edited by D. Thomas (Benjamin, New York, 1967), p. 503.

[23] H. Overhof (private communication).

[24] R. Hengehold, R. Almassy, and F. Pedrotti, Phys. Rev. B 1, 4784 (1970).

PHYSICAL REVIEW B VOLUME 4, NUMBER 2 15 JULY 1971

Electron-Irradiation Effects in Silicon at Liquid-Helium Temperatures Using ac Hopping Conductivity*

R. E. McKeighen and J. S. Koehler

Nuclear Engineering Program, Department of Physics, and Materials Research Laboratory,
University of Illinois, Urbana, Illinois 61801

(Received 25 February 1971)

Changes in ac hopping conductivity with electron irradiation have been measured in n-type, p-type, and high-purity silicon. Irradiations were carried out at both 5.0 and 1.6 °K, with measurements made at reference temperatures of 4.2 and 1.3 °K, respectively. In the p-type crystals, the changes in ac hopping conductivity depend strongly on the concentration of chemical acceptors, indicating a concentration dependence on impurities in the defect production rate. The production rates at 1.6 °K were generally very similar to those for a 5.0 °K irradiation. No significant thermal annealing stages below room temperature were observed in any of the crystals. No radiation annealing effects due to a beam of either 0.500-MeV or 0.350-MeV electrons were observed, either at 4.5 or 1.45 °K. The possibility of athermal effects leading to interstitial migration is suggested.

I. INTRODUCTION

Radiation effects in semiconductors, particularly silicon and germanium, have been studied since the early 1950's. Early research had two motivating emphases: (i) determining defect yields resulting from exposure to a variety of radiations in order to check the simple theory of defect displacements; (ii) constructing defect models to account for the multitude of energy levels produced in terms of simple Frenkel defects. Although this field has not suffered from lack of experimental data, some of the most fundamental questions are still being asked. (a) What are the impurities? (b) What moves at the lowest irradiation temperature, and what is that temperature? (c) Where is the interstitial? (d) What is the configuration of the interstitial?

Watkins's[1] EPR measurements indicated that the vacancy in p-type silicon is mobile in the temperature range around 160 °K and that the vacancy in n-type silicon is mobile in the range 60–80 °K.

The self-interstitial in silicon has never been observed. It is believed to be mobile even during a liquid-helium-temperature irradiation because of the following observation made by Watkins. Isolated vacancies and interstitial aluminum atoms (Al^{++}) were produced in approximately 1 : 1 correspondence (~0.03 defects/cm^3 per electron/cm^2) by 1.50-MeV electron irradiation. Now, for every vacancy formed in a primary radiation damage event, there must also be an interstitial atom. Watkins suggested that the interstitial silicon atom migrates through the lattice until trapped by the substitutional aluminum atom. In the trapped state, the silicon atom replaces the substitutional aluminum atom, ejecting it into the interstitial site. The end result is a vacancy and an interstitial aluminum atom well separated from each other.

The motivation for the present experiment was to see if the interstitial is indeed mobile during a liquid-helium-temperature irradiation using some observation different from EPR. The difficulty in silicon is that normal electrical measurements depend on free carriers in the crystal; they are frozen out at temperatures below about 30–40 °K so that dc electrical conductivity becomes very small. Measurement of ac hopping conductivity, however, can be made down to below 1 °K. The present measurements show that ac hopping conductivity can be used as a tool for studying radiation effects in silicon.

II. DISCUSSION OF ac HOPPING CONDUCTIVITY

If one considers a crystal doped with only one kind of impurity, say, n-type impurities of concentration N_d, at $T = 0$ °K, all of the electrons that are thermally excited from the donors into the conduc-